Quartz grain features in modern glacial and proglacial environments: A microscopic study from the Russell Glacier, southwest Greenland

Edyta KALIŃSKA-NARTIŠA[1, 2*], Kristaps LAMSTERS[3], Jānis KARUŠS[3], Māris KRIEVĀNS[3], Agnis REČS[3] and Raimonds MEIJA[4]

[1] *SunGIS SIA, Pruuni, Rencēni Parish, Burtnieki region, LV-4232, Latvia*

[2] *University of Tartu, Institute of Ecology and Earth Sciences, Department of Geology, Ravila 14A, EE-50411 Tartu, Estonia*
<edyta.kalinska@gmail.com>

[3] *University of Latvia, Faculty of Geography and Earth Sciences, Jelgavas street 1, LV-1004, Riga, Latvia*
<kristaps.lamsters@gmail.com> <janis.karuss@inbox.lv>
<maris.krievans@gmail.com> <agnis.recs@gmail.com>

[4] *University of Latvia, Institute of Chemical Physics, Jelgavas street 1, LV-1004, Riga, Latvia*
<raimonds.meija@lu.lv>

* corresponding author

Abstract: It is assumed that close to the margins of ice-sheets, glacial, fluvial and aeolian processes overlap, and combined with weathering processes, produce numerous sediments, in which quartz is a common mineral. Quartz grains, if available, may serve as a powerful tool in determining the depositional history, transportation mode and postdepositional processes. However, quartz grain studies in some modern glacial areas are still sparse. In this study, we examine for the first time quartz grains sampled from the modern glacial and proglacial environments of the Russell Glacier, southwest Greenland in binocular microscope and scanning electron microscope, to analyze their shape, character of surface and microtextures. We debate whether the investigated quartz grains reveal glacial characteristics and to what extent they carry a signal of another transportation and sedimentary processes. Although glacial fracturing and abrasion occur in grain suites, most mechanical origin features are not of a high frequency or freshness, potentially suggesting a reduced shear stress in the glacier from its limited thickness and influence of the pressurized water at the ice-bed. In contrast, the signal that originates from the fluvial environment is much stronger derived by numerous aqueous-induced features present on quartz grain surfaces. Aeolian-induced microtextures on grain surfaces increase among the samples the closest to the ice margin, which may be due to enhanced aeolian activity, but are practically absent in sediments taken from the small

scale aeolian landforms. In contrast, aeolian grains have been found in the bigger-size (1.0–2.0 mm) investigated fraction. These grains gained the strongest aeolian abrasion, possibly due to changes in transportation mode.

Introduction

Modern glacial environments provide insight into subglacial conditions and processes through its fresh sedimentological record (*e.g.* Knight 1997; Adam and Knight 2003; Cook *et al.* 2011). Such records can be obtained, for example, from sediments deposited during melt-out of former ice masses and further preserved close to the ice margin (*e.g.* Baltrunas *et al.* 2008). In these sediments, not only glacial record, but also signal of fluvial (Karlstrom and Yang 2016) and/ or aeolian processes (Müller *et al.* 2016) may be expected.

Under cold-climate conditions, ice acts as a weathering and eroding agent, triggering rock disintegration and preferentially producing quartz grains (Schwamborn *et al.* 2012), except of areas, where quartz is not available. Quartz grains are highly resistant to weathering and thus remain in the sedimentary environment (Krinsley and Doornkamp 1973; Mahaney 2002) and may record sedimentary processes (Newsome and Ladd 1999; Moral Cardona *et al.* 2005; Konopinski *et al.* 2012; Vos *et al.* 2014), identify mode of transport (Kleesment 2009) or estimate duration of processes modeling the grains (Krinsley and Doornkamp 1973; Refaat and Hamdan 2015).

In this study, we examine grain shape, surface character and micromorphology (=microtexture) of quartz grains from the sand fraction of deposits around the Russell Glacier, South West Greenland (Fig. 1). This area is characterised by excellent landform preservation (Ten Brink 1975; Česnulevičius and Šeirienė 2009; Šinkūnas *et al.* 2009), and combined with its accessibility, make it ideal for a new quartz grain study. Our samples represent numerous settings (=landforms) such as sandur plain, dune/coversand, lake terrace, end moraine and many more, for more details see Table 1 and Figs. 1, 2. By using proxies that originate from these settings, which are closely related to the Russell Glacier, we provide an insight into sedimentary record of the modern glacial and proglacial environments and define sediment transformation under such conditions. We thus aim in answering the following research questions: (1) whether these quartz grains reveal glacial characteristic, and (2) what kind of other grain features (that may originate from any other sedimentary processes) does the grains exhibit?
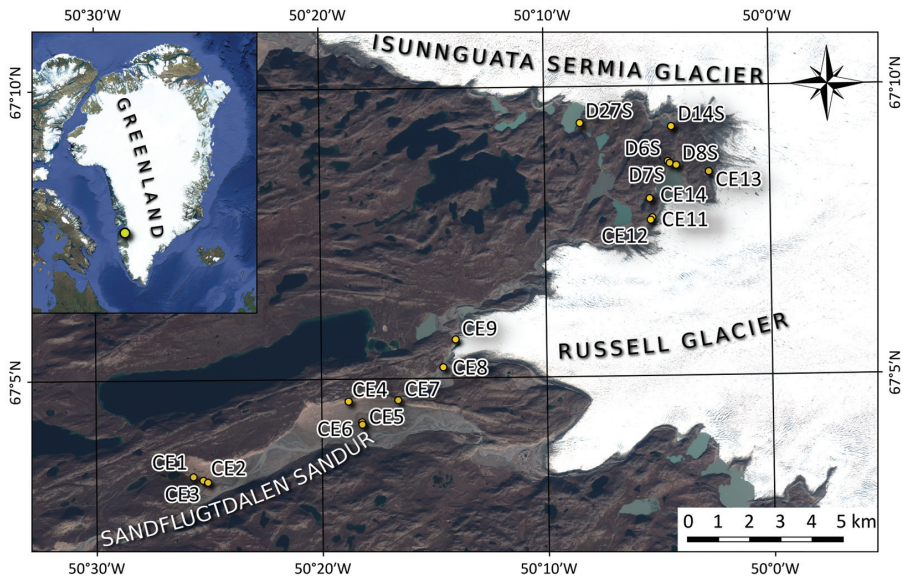
Fig. 1. Location of the investigated area and sampling points.

Study area

We focus our studies on the Kangerlussuaq-Russell Glacier area, South West Greenland, which represents the largest ice-free area in Greenland (Funder and Hansen 1996). In the Holocene, retreats of the Greenland Ice Sheet (GrIS) margin were interrupted by numerous re-advances, which are evident from the moraine ridges as Fjord, Umîvît, Keglen and Ørkendalen with established geochronology (Carrivick *et al*. 2016). The Ørkendalen moraine system reflects one of the major glacial advance prior the Little Ice Age (LIA), which took place between 6400 and 7030 cal. years BP according to radiocarbon datings (Storms *et al*. 2012). The other possible advance could have culminated at ~2.0 cal. years BP (Forman *et al*. 2007), but further investigations are needed to support this statement (Storms *et al*. 2012). During the past 20 years, the mass balance of the GrIS is negative, and recent warming in the western part of the GrIS has increased melt extent, surface runoff and discharge (Van As *et al*. 2012).

The Archaean ortho-gneisses comprising the southern part of the Nagsugtoqidian Orogen are the main bedrock constituent of the Kangerlussuaq-Russell area (Van Gool *et al*. 2002). Bedrock depressions were glacially eroded, forming U-shaped valleys, and subsequently partially filled, usually with sandy till (Aaltonen *et al*. 2010). For example in the Sandflugtdalen study area (Fig. 1) 50–80 m thick sedimentary infill exists, represented by ice-contact, deltaic and glaciolacustrine deposits (Storms *et al*. 2012).

Table 1

Sample information including the sampling site with its location
and geomorphological/sedimentological description.

No.	Location	Description
CE1	Embryonic dune	Sample from one of small-scale embryonal dunes in the distal part of sandur. Dunes have developed on the gently sloping hillslope and are associated with sparse vegetation cover (small grasses and shrubs).
CE2	Coversands in distal sandur	Sample taken little further away from small-scale dune field, where the flat sandur surface is affected by wind forming coversands. Surface covered by wind ripples.
CE3	Distal sandur	Exposed coarse sand ripples near the active stream.
CE4	Echo dune accumulated atop of scarp	Aeolian sands on a steep valley slope in middle part of sandur. Crystalline rocks (gneiss) are exposed at higher level, and sand seems to be blown directly on bedrock slope.
CE5	Middle sandur	Sand ripples in the middle sandur floodplain. Very sparse vegetation grows in some depressions between ripples.
CE6	Middle sandur	Exposed bar near to the main channel (active). Surface is covered by pebbles and cobbles.
CE7	Transition zone between middle and proximal sandur	Sample from horizontally bedded sand, where the main stream channel from the Russell glacier encounters braided streams from the Leverett glacier. Horizontally bedded sands are underlain by cross-bedded sands. Crystalline rocks constrain channel from sides.
CE8	Proximal sandur	Proximal sandur 400 m from Russell margin. Sample from the floodplain near main channel. Little Ice Age end moraine is located at the opposite bank. Sand and gravel occur between large boulders and are reworked by wind action.
CE9	Flood channel	Sample from relict channel near the margin of the Russel glacier. Proglacial stream has eroded large niche in the steep ice margin. Course material with boulders is exposed at the channel bed, and fallen icebergs can be found closer to ice margin.
CE11	Aeolian cover on end moraine	Fine sand sediments taken form terrace-like surface on the middle part of end moraine at the ice margin (see CE12 description). Sediments are apparently aeolian origin and overlie till up to few tens of centimetres in thickness.
CE12	End moraine	Sandy till sediments from the middle part of the end moraine that fit close to the hillslope. Possibly melt-out till sediments are found on the hillslope up to 40 m higher that present ice surface. The upper part of the moraine most likely represents Little Ice Age End moraine, while the lower part is ice-cored and active hillslope processes are occurring. Sample is taken 20 m away from ice margin.

Table 1 continued

No.	Location	Description
CE13	Supraglacial debris	Supraglacial debris 20 m away from ice margin. The Little Ice Age end moraine is near present ice margin. Debris is re-worked by small and very shallow supraglacial streams that cover almost all ice surface.
CE14	Lake terrace	Sample from an ice-dammed lake terrace close to the high water mark. Sandy and gravely sediments almost without vegetation are concentrated in up to 2 m wide zone near the former shorline. Cobbles and boulders form pavement on the former lake bottom. The highest water level is periodically reached in jökulhlaup events. During jökulhlaups water is drained through subglacial tunnel and passageway that connects this ice-dammed lake with lake located at lower topographical level. Lake passageway is few tens of meters away from sampling site.
D6S	Aeolian cover on a hillslope	Aeolian sands on a hillslope close to the ice-dammed lake.
D7S	Lake terrace	Sands from ice-dammed lake terrace.
D8S	Lake shoreline	Sands near present shoreline of a ice-dammed lake.
D14W	Distal part of proglacial delta.	Sands from distal part of delta in proglacial lake that is dammed by the Little Ice Age end moraine. Present-day ice margin is close to the end moraine. Lake is drained by river between ice margin and end moraine (through incision in this end moraine). Delta is active and rapid streams are flowing into the lake, although water level is several meters below high water mark. Three terrace levels are recognizable.
D27W	Lake shoreline	Sands near present shoreline in a bay of ice-dammed lake. Crystalline basement and till is exposed on banks.

Our fieldwork took place in two areas. The first locates between Isunnguata Sermia Glacier, representing the deepest subglacial trough system (Lindbäck *et al*. 2014), and the Russell Glacier (Fig. 1). Here, several settings as a lake terrace, shoreline, delta, hillslope, along with ice surface and end-moraine, occur and these landforms were observed and sampled (*see* Fig. 2 for details). Wind-blown silt covers end moraines on some terrace-like surfaces close to the ice margin, and ice surface itself is very dark and covered by dust, although light-coloured linear and very shallow channels stretches across the ice surface suggesting fluvial reworking of mineral particles.

The second area is along the Sandflugtdalen sandur (Figs. 1 and 2) that fills the northern branch of the valley basin, stretching a distance of 25 km between the terminus of the Kangerlussuaq Fjord (Søndre Strømfjord) and the GrIS margin (Storms *et al*. 2012). This sandur is fed by the proglacial streams of the Russell
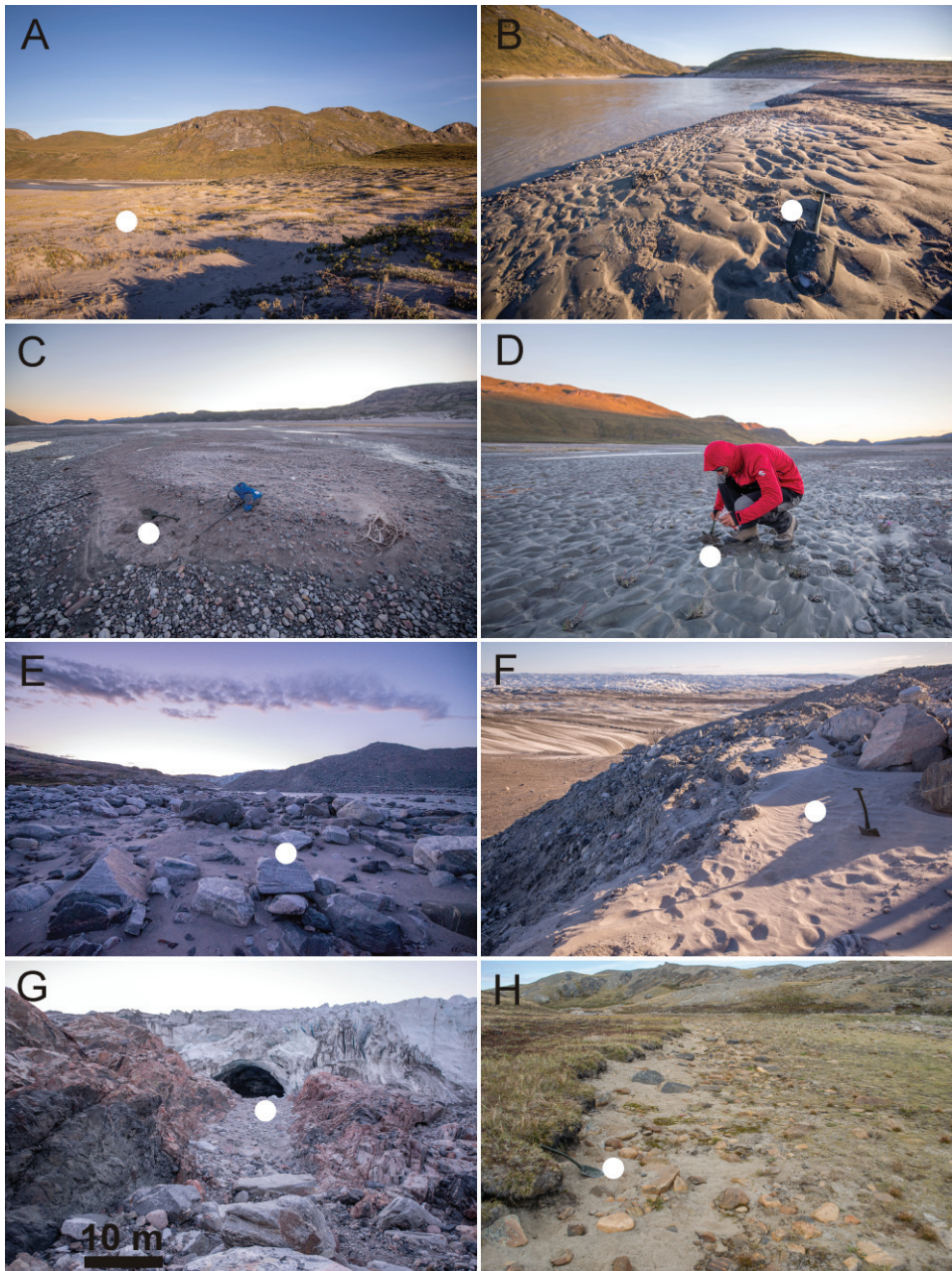
Fig. 2. Examples of sampled settings. (**A**) Embryonic dune; (**B**) Distal sandur (sand ripples); (**C**) Middle sandur (exposed bar); (**D**) Middle sandur (sand ripples); (**E**) Proximal sandur (floodplain near main channel); (**F**) End moraine and aeolian cover on it; (**G**) Flood channel; (**H**) Lake terrace. White circles show sampling locations.

and Leverett glaciers, and drained by the Watson River, in which catastrophic Jökulhlaup events are recorded (Russell 2007, 2009; Česnulevičius *et al*. 2009; Russell *et al*. 2011) with a frequency of every 2–3 years between the 1950s and 1987 (Russell 1989). The area related with the Sandflugtdalen sandur provides an opportunity not only to study sand grains from different sandur zones, but to estimate aeolian impact, because the floodplain is characterised by enhanced wind activity and formation of small-scale dunes. The aeolian silt covers also valley slope in middle part of sandur and nearby hilltops and slopes as well, where crystalline bedrock (gneisses) is not exposed.

The Kangerlussuaq area, situated in the rainshadow of the Sukertoppen icecap, receives annual precipitation average of 150 mm/y (Engels and Helmens 2010). Annual mean temperature at Kangerlussuaq airport is -5.7°C as measured in 1973–99 period (Cappelen *et al*. 2001). Since the beginning of 1990s, the air temperature has increased by 2–3°C, however, the mean annual air temperature is still below -4°C (Jørgensen and Andreasen 2007). Mean wind speed at 2 m above ground level is 3.6 m/s (years 1985–99; Cappelen *el al*. 2001). Due to the aforementioned conditions, this area may be regarded as a polar desert. Since the study area is directly linked to the ice, it is probably drier and colder and more influenced by winds (*see also* Müller *et al*. 2016).

The investigated area is located in the southern part of the continuous permafrost zone, which close to the ice margin reaches up to 350–400 m in thickness (Liljedahl *et al*. 2016). This has resulted in numerous periglacial features in lowlands, such as patterned ground, hummocks and ice-wedges, erratics with honeycomb weathering and occurrence of loess (Aaltonen *et al*. 2010).

Methods

Fieldwork was carried out in June and August 2016, when eighteen sediments samples were taken from numerous landforms (Fig. 2, Table 1). These samples were collected in plastic bags and further oven dried at 105°C. Around 100–150 g of subsamples were mechanically sieved for 15 min according to recommendation of Román-Sierra *et al*. (2013). Two sand fractions (0.5–1.0 mm and 1.0–2.0 mm) were picked up, etched in HCl to remove possible carbonates and thoroughly washed.

To analyze both the degree of quartz grain rounding and the type of surface, a binocular microscope with magnification of 40x was used, and *ca*. 100 (the first method below) as well as *ca*. 50 quartz grains (the second method) were analysed. We employed two methods: (1) following Cailleux (1942) and modified by Mycielska--Dowgiałło and Woronko (1998) for the 0.5–1.0 mm fraction, and (2) after Velichko

and Timirieva (1995) for the 1.0–2.0 mm fraction. Both methods combine few classes of roundness (well-rounded, moderately rounded and non-abraded in the first method; classes 0 to IV, where 0 – non-abraded and IV – rounded in the second method) with few classes of grain surface (matt, shiny in the first method; shiny, quarter-matt, half-matt and matt in the second method). Finally, a roundness (Q) and dullness (F_m) coefficients were calculated following the formulas proposed by Velichko and Timirieva (1995). Although larger (>0.5 mm) particles may be pushed or rolled along the surface rather than saltated (Nickling and McKenna Neuman 2009), wind action is best visible in grain ~0.7 mm (Cailleux 1952).

A total of 100 grains, belonging to 5 samples (20 grains per sample), were randomly selected and prepared for analyses by scanning electron microscope (SEM). We use Hitachi FE-SEM S-4800 at the University of Latvia and Zeiss EVO MA 15 at University of Tartu. The samples represent the following settings: (1) embryonic dune (sample CE1), (2) coversand (sample CE2), (3) proximal part of sandur (sample CE8), (4) end moraine setting from the Little Ice Age (sample CE12), and (5) supraglacial debris (sample CE13). We considered these samples as giving an overall picture of the study area. Grains were positioned in rows onto a double-sided carbon tape on top of a SEM holder and gold-coated. Grains were imaged with *ca*. 100x magnification to determine roundness (rounded, subangular, angular), relief of grains and their general outline, and *ca*. 300–1200x magnification to determine presence of microtextures. The microtexture classification followed the proposal of Mahaney (2002) with supplementations taken from an earlier study by Goudie and Bull (1984). Raw data is available in Table 3. Partially following the methods of Vos *et al*. (2014), the types of microtextures, as of mechanical, chemical and combined origin, together with a general grain outline have been semi-quantified based upon their occurrence (= frequency distribution, in which the statistics are based on the number of grains exhibiting a specific microtexture within a sample) as abundant (>75%), common (50–74%), medium (26–49%), sparse (6–25%), rare (<5%) and not observed. Finally, we grouped microtextures of mechanical origin as high-stress, percussion and polygenic features (Sweet and Soreghan 2010), and further calculated the ratio of fluvially to glacially induced microtextures (F/G) according to proposal of Sweet and Brannan (2016).

Results

Quartz grain roundness and type of surface according the Cailleux's analyses. — Under the binocular magnification, fresh grains with sharp edges and shiny surface (=non-abraded) are important constituents in most of the investigated samples (Fig. 3) with the highest value of 78% in the D6S sample, which represents aeolian cover on a hillslope (Table 1). Grains with sharp edges are followed in the investigated samples by roughly equal percentages of moderately rounded grains
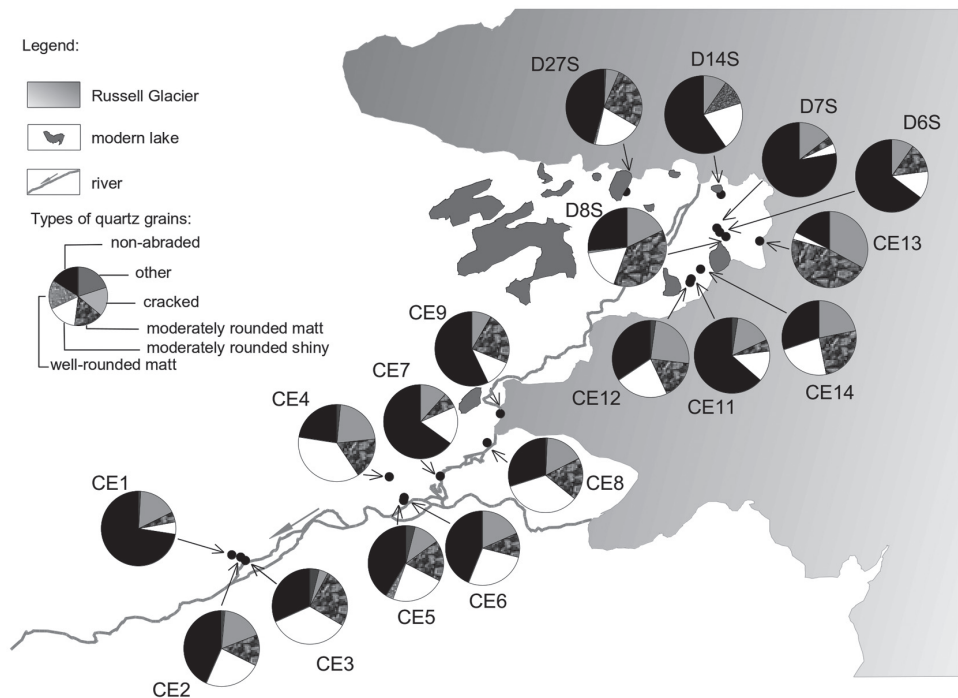
Fig. 3. Spatial distribution of quartz grain (0.5–1.0 mm) roundness and type of surface, distinguished according to Cailleux (1942) with modification of Mycielska-Dowgiałło and Woronko (1998).

with shiny surface (5–27%), moderately rounded grains with matt surface (3–27%) and cracked grains, which lack at least 30% of their original surface (6–25%).

In three sediment samples taken from the distal part of sandur, cover sand and echo dune (CE3, CE2 and CE4, respectively) moderately rounded shiny grains are as high as 34–37% (Fig. 3). Moderately rounded grains with matt surface prevail in two samples: in the supraglacial debris (sample CE13; 46%) and sediment from the lake shoreline (sample D8S; 38%). In the latter, fresh and cracked grains occur (26% and 18%, respectively; Fig. 3). In contrast, in the supraglacial debris cracked grains predominate at 33%, followed by fresh grains at 18%.

Quartz grain roundness and type of surface according the Velichko's and Timirieva's analyses. — The 1.0–2.0 mm fraction is dominated by shiny quartz grains with the lowest degree (the zero and the first classes) of roundness (between 0% and 32%, and 0–60%, respectively; Fig. 4). Quarter-matt grains from the first class of roundness vary between 0% and 42%. Such grain combination equate to relatively low mattness (F_m) and roundness (Q) coefficients, which vary between 2% (samples CE6 and CE8) and 24% (sample CE4), and between 11% (sample CE8) and 28% (sample CE2), respectively (Table 2). However,
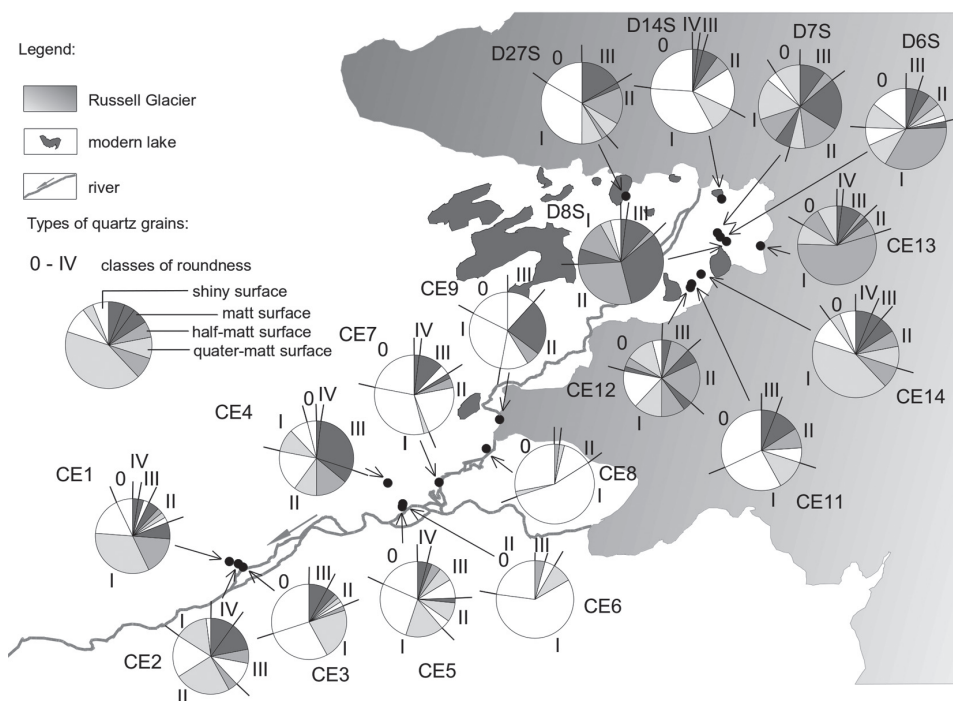
Fig. 4. Spatial distribution of quartz grain (1.0–2.0 mm) roundness and type of surface, distinguished according to Velichko and Timirieva (1995).

samples representing sediments from the lake terrace (D7S) and lake shoreline (D8S), and supraglacial debris (CE13) reveal a F_m value up to 35%, indicating that matt grains from the second and third roundness classes prevail. Up to 10% of well-rounded (the IV roundness class) matt grains have been observed in the sandur setting from its distal part (sample CE2).

Quartz grain roundness and surface microtextures in the SEM. — Most grains investigated in the SEM are subrounded either with a number of edge rounding (Figs. 5 and 6A; Table 3), or associated with both edge rounding and big conchoidal features (Figs. 5 and 6B). This latter type of grain may correlate to the cracked grains utilizing the Cailleux's methodology. In contrast, angular (Fig. 6C) and rounded grains occur sparsely, rarely or have not been found (Fig. 5). Either medium (Figs. 5 and 6D; Table 3) or low grain relief (Figs. 5 and 6E; Table 3) prevail. In contrast, high relief is either sparse (Fig. 6F) or not observed.

Among mechanical microtextures, the most popular are big- and medium-size conchoidal features (Figs. 7A and B, respectively), which occur either abundantly or commonly. Small-size conchoidal features are also present (Fig. 6B). These conchoidals are almost always accompanied with numerous arcuate (Fig. 7C)

Table 2

Selected results of the quartz grain roundness and dulness, and microtextures
on its surface. F/G ratio refers to fluvially (F) and glacially (G)
induced microtextures.

Sample no.	Binocular		SEM			
	Roundness coefficient (Q)	Mattness coefficient (F_m)	Polygenic features [%]	Percussion features [%]	High-stress features [%]	F/G ratio
CE1	15	17	66	21	14	2
CE2	28	19	76	22	2	9
CE3	12	10	–	–	–	–
CE4	25	24	–	–	–	–
CE5	18	9	–	–	–	–
CE6	12	2	–	–	–	–
CE7	18	8	–	–	–	–
CE8	11	2	73	16	11	2
CE9	18	19	–	–	–	–
CE11	14	26	–	–	–	–
CE12	13	12	75	20	5	4
CE13	16	21	60	36	4	8
CE14	16	18	–	–	–	–
D6S	13	20	–	–	–	–
D7S	20	29	–	–	–	–
D8S	24	35	–	–	–	–
D14W	14	9	–	–	–	–
D27W	18	15	–	–	–	–

– not analysed

or straight steps (Fig. 7D). Dulled surface is abundant on grains from the CE13 sample (82%; Fig. 7E) and associated with the V-shaped percussion cracks (35%; Fig. 7F). In general, meandering ridges, breakage blocks, straight/curved grooves and crescentic marks occur sparsely, rarely or were not observed (Figs 5, 8A, B, C, respectively). Chattermarks are also sparse (samples CE2 and CE8; Fig. 8D). Importantly, some of the mechanical microfeatures seem to be "old" and overprinted *i.e.* by adhering particles (Fig. 7F) and precipitation (Fig. 8E), which likely occurs in all depressions (Fig. 8E). Grains with solution pits and crevasses (Fig. 8F) reveal wide variety of occurrence (Fig. 5).

The group of mechanical microtextures of polygenetic origin dominates in all investigated samples and vary between 61% and 73% (Table 2). The second most common are percussion microtextures, whereas the high stress features stay in the minority (2–4%). Fluvially induced microtextures dominate significantly over glacially induced. This is apparent from the F/G ratio, which differs between 2 and 5 (Table 2).
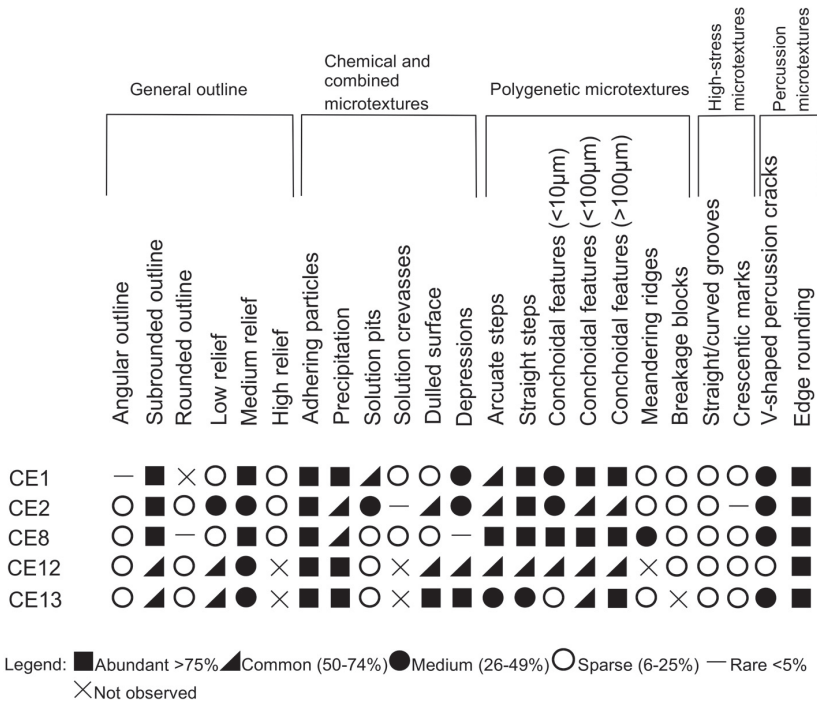
Fig. 5. The occurrence of the quartz microtextures of mechanical, chemical and mechanical-chemical origin.

Discussion

Our results reveal that three potential sedimentary environments (glacial, fluvial and aeolian) may have contributed in deposition of debris related to the Russell Glacier and its meltwaters (Fig. 9). We discuss these potentials in the following sections.

Glacial environment. — Since the study area has experienced at least five glacial episodes in the Holocene (Carrivick *et al.* 2016), we expected grain outline associated with ice action, where grain-to-grain contact along existing shear planes can result in one grain stylizing microtexture onto another grain (Sweet and Brannan 2016). Glacial erosion acts, therefore, either by fracturing or abrasion (Whalley and Langway 1978), and thus producing grains of high angularity or, conversely, with a different level of abrasion (Mahaney *et al.* 1996; Hart 2006). This study shows that glacial-driven grains are certainly present (Fig. 8), because most our samples, observed in the binocular, shows a combination of (1) angular, which may correspond with the shiny and quarter-
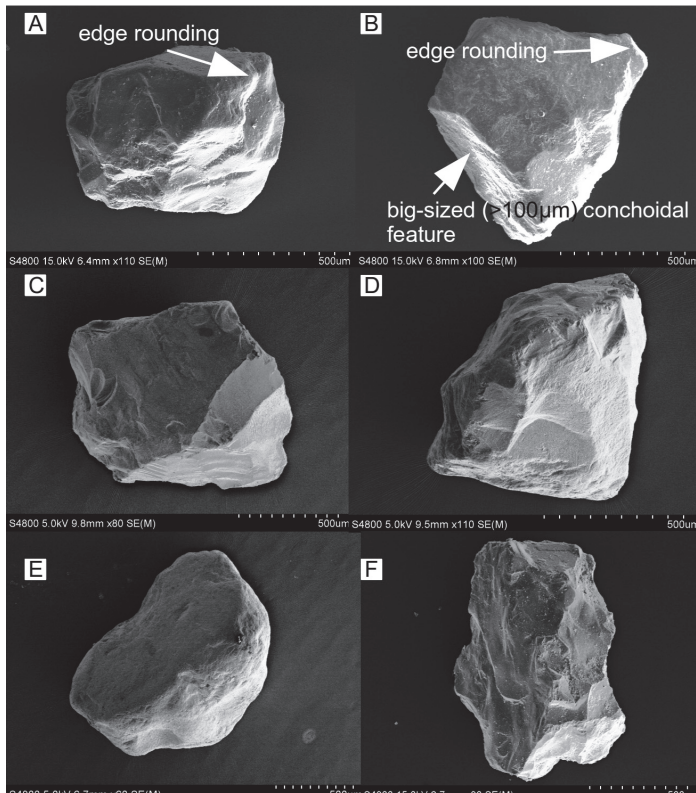
Fig. 6. Explanatory images of quartz sand grain features. (**A**) subangular grain with edge rounding; (**B**) subangular grain with edge rounding and big-sized (>100 μm) conchoidal feature; (**C**) angular grain; (**D**) grain with medium relief; (**E**) grain with low relief; (**F**) grain with high relief.

matt grains from the class 0 in the 1.0–2.0 mm fraction; (2) cracked, which partially represents the shiny/quarter-matt grains from the II class; and (3) shiny with different degree of rounding grains, *i.e.* shiny and quarter-matt from the I–IV classes, however the I class dominates. Contrary to the observation of Muzińska (2015), we have not noted predominance of so called "other" quartz grains with surfaces of intense precipitation and etching formed due to chemical weathering (Woronko *et al*. 2015a). Such grains are practically absent at the field area; however, precipitation itself has been observed all across the grain surfaces in the SEM imagery, and may result from glacial conditions (see below).

Binocular observations of two different sized sandy fractions by two binocular methods likely coincide with each other; shiny grains with relatively low roundness (non-abraded) prevail in the 0.5–1.0 mm fraction and shiny (and quarter-matt) grains from the 0 and the I classes dominate in the 1.0–2.0 mm fraction. However, the general grain-shape properties in both the binocular and the SEM observations slightly differ. Grains with a number of conchoidal features
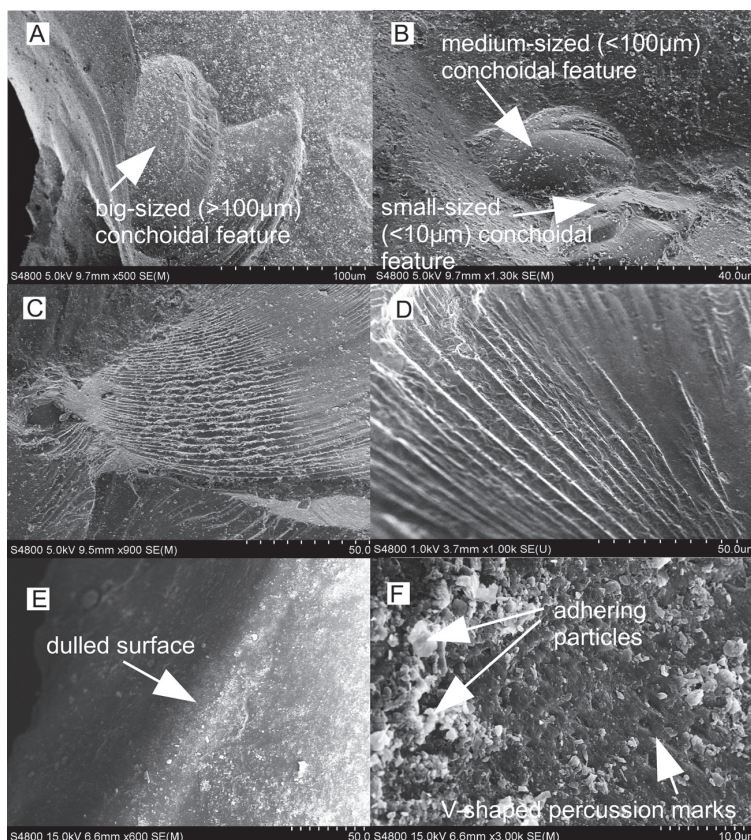
Fig. 7. Explanatory images of quartz surface microtextures. (**A**) big-sized (>100 μm) conchoidal feature; (**B**) medium- (<100 μm) and small-sized (<10 μm) conchoidal features; (**C**) series of arcuate steps; (**D**) series of straight steps; (**E**) dulled surface on the most concave part of grain; (**F**) V-shaped percussion marks and adhering particles.

of different size dominate in the SEM, but also most of these grains exhibit bulbous edges, which classify as subangular grains. Therefore, it seems that bulbous edges are visible only under the SEM, and under weaker binocular's magnification these grains resemble a non-abraded wear.

Apparent from the SEM imagery is that most of grains carry either medium or low relief (Fig. 5; Table 3). This is in contrast with the high relief, which belongs to the most recognisable glacial features (Immonen 2013) among microtextures caused by high-pressure fracturing during glacial transport such as straight and curve grooves, and chattermarks (Mahaney and Kalm 1995; Mahaney 2002; Mahaney *et al*. 2004; Sweet and Soreghan 2010; Kirshner and Anderson 2011; Vos *et al*. 2014; Mazumder *et al*. 2017). Analysed grains, due to their minor fracturing (*see* high stress features in Table 2) and medium/low relief (Fig. 5), may record scenarios as proposed by Mahaney and Kalm (1995)

Table 3

Number of investigated grains per sample along with number of grains
that exhibit the microtexture.

| Sample	CE1	CE2	CE8	CE12	CE13
Total	20	20	20	20	20
Conchoidal (<10 μm)	8	9	19	11	3
Conchoidal (<100 μm)	16	11	19	13	11
Conchoidal (>100 μm)	15	11	15	12	14
Chattemarks	0	3	1	0	0
Arcuate steps	13	12	16	13	7
Straight steps	16	17	15	13	6
Meandering ridges	7	3	6	0	1
Graded arcs	1	2	0	0	0
V-shaped cracks	6	6	6	4	6
Straight/curved grooves	2	3	4	3	2
Crescentic marks	4	1	3	2	3
Bulbous edges	19	15	16	18	17
Abrasion fatigue	5	3	6	5	1
Parallel striations	2	4	6	5	3
Oriented etch pits	2	0	0	0	0
Solution pits	12	6	4	3	6
Solution crevasses	5	1	2	0	1
Silica pellicle	0	0	0	2	2
Crystalline overgrowths	0	1	0	3	1
Precipitation	18	10	12	18	17
Dulled surface	5	14	3	10	14
Breakage blocks	4	3	2	2	0
Low relief	2	7	2	13	14
Medium relief	16	9	16	7	6
High relief	2	4	2	0	0
Depressions	9	8	1	14	7
Adhering particles	20	19	20	20	20
Angular grains	1	4	3	2	1
Subangular grains	19	15	16	13	17
Rounded grains	0	2	1	5	2
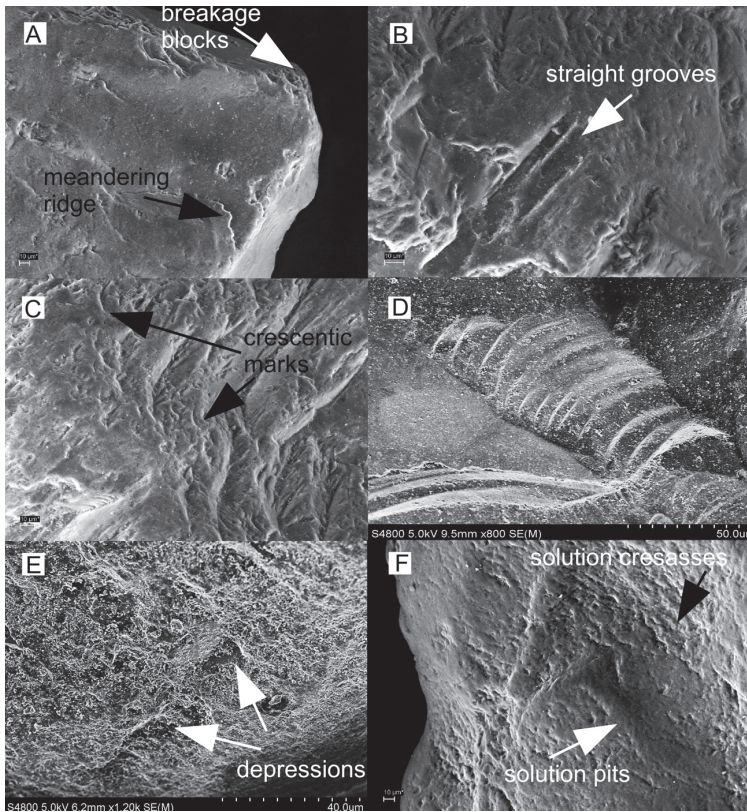
Fig. 8. Explanatory images of quartz surface microtextures. (**A**) breakage blocks on the most concave part of grains and meandering ridges; (**B**) straight grooves; (**C**) crescentic marks; (**D**) chattermark; (**E**) very intense silica precipitation covering all grain surface including depressions; (**F**) solution pits and solution crevasses.

and Shrivastava *et al.* (2012). In the first scenario, grains were incorporated to the glacier from non-glacial source; whereas, in the second scenario, grains solely experienced glacial transported over a short distance. These two schemes may also be proposed for other grain mechanical features, such as step microtextures, which are produced both in the fluvial (Udayaganesan *et al.* 2011) and glacial environments (Strand *et al.* 2003). This combination implies that grains may be derived from the crystalline source rocks (Madhavaraju *et al.* 2006), or indicate sediment short transportation and rapid deposition (Gobala Krishnan *et al.* 2015). Following this knowledge, steps are of polygenetic origin (Sweet and Soreghan 2010) and their occurrence may lead to ambiguous interpretations. In such situation, the F/G ratio helps by showing that signal coming from the fluvial (subglacial?) environment is much stronger, than recorded by the glacial environment (Table 2). Similar doubts about importance of the glacial influence
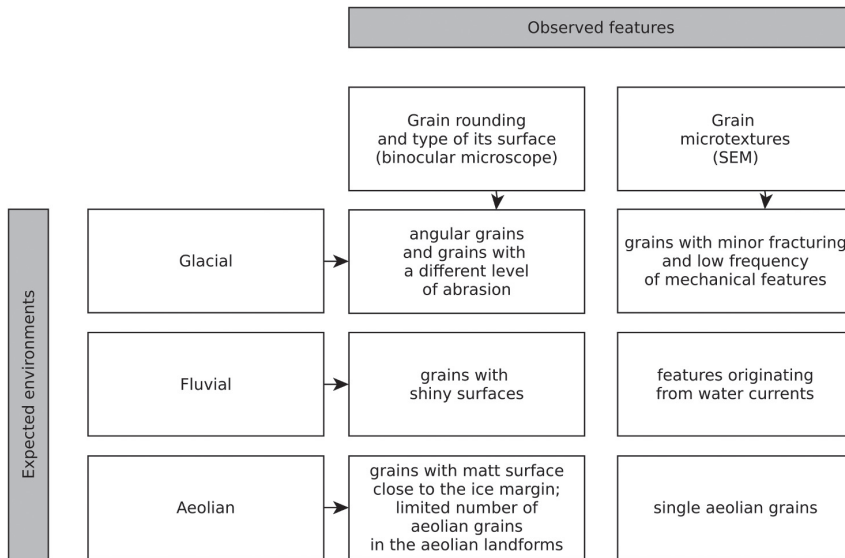
Fig. 9. Sedimentary environments contributing in deposition at the Russell Glacier as obtained from the quartz grain shape, character of its surface and micromorphology.

in the proglacial realm were also raised by Clarhäll (2011), who concluded that sediment dynamics is rather governed by non-glacial processes, predominantly fluvial and aeolian. In this study, most high stress origin features on quartz grain surfaces are not well-expressed, which points at reduced shear stress in the glacier. This agrees with observations of Mahaney (2002), who stated that smaller glaciers and ice caps transport sediments in a lower stress regime as opposed to large ice sheets which transport grains with higher stress. If so, at least *ca*. 500 m thick ice is needed to produce the most recognisable glacial high-pressure fracturing (Mahaney *et al*. 1996). Therefore, only minor fracturing and abrading might be subjected, for example, to alpine glaciers with an estimated ice thickness of less than 200 m (Mahaney 1995), to the Saalian and late Weichselian tills in Poland (Woronko 2016; Kalińska-Nartiša *et al*. 2017), modern sea-ice rafted sediments (St. John *et al*. 2015) and even to the surge glacier (Muzińska 2015). Certainly, studied grains underwent only a limited resurfacing in the marginal part of the glacier, thus its impact was not strong enough to produce a set of high stress microfeatures. Another explanation may be due to a presence of pressurized subglacial water (Aaltonen *et al*. 2010), which reduces inter-granular contact within the sediment, and/or extreme jökulhlaup events (*see* Aqueous signal?).

Nevertheless, ice conditions may have contributed to the development of chemically induced and combined microtextures indicated by abundance of adhering particles (Fig. 5), and precipitation either in depressions or occasionally

on an entire grain surface. These microtextures are another evidence for glacial environment, in which debris were trapped in the ice (Immonen 2013) or/and resulted from the glacial grinding (Whalley and Langway 1978).

Aqueous signal. — Since the modern glacial environment is strongly linked with highly dynamic meltwater regimes including episodes of extremely intense runoff (Carrivick *et al*. 2016), a number of aqueous-induced textures on the quartz grains should be considered. These are rounded outlines, low reliefs and impact v-shaped marks (Mahaney 1998; Mahaney and Kalm 2000; Madhavaraju *et al*. 2006), which are produced during grain-on-grain impact in low-viscosity media (Sweet and Brannan 2016).

In our study, most samples contain a significant number of grains with shiny polished surfaces and different degree of rounding (Fig. 6, Table 2), which tend to be produced under energetic fluvial conditions (Nanson *et al*. 1995; Kleesment 2009; Vos *et al*. 2014). More fluvial-induced grains can be found, for example, in the sandur sediments. Large amount of this sediment originates from the highly energetic jökulhlaup events (Russell 1989, 2007, 2009; Česnulevičius *et al*. 2009; Russell *et al*. 2011). Significant runoff may start in May and end in September (Liljedahl *et al*. 2016), thus providing a new influx of silt and sand (Engels and Helmens 2010) during a 3–4 month season. We have, however, not observed a high-energetic grain transformation towards its distal part likely due to too short transportation distance. Fluvial grains from a proximal and distal part of sandur reach a similar level (in the 0.5–1.0 mm fraction), or are replaced by aeolian-induced grains in the 1.0–2.0 mm fraction; see the next chapter. This latter is likely due to deposition under alternating humid-dry conditions as observed in the Late Glacial palaeoenvironments (Kalińska-Nartiša and Nartišs 2016).

Under SEM, individual grains taken from the supraglacial debris and coversand, display limited high-impact features that originate from the glacier itself. Rather, these grains reveal predominant features normally attributable to water currents (Fig. 9). For example, many of the surfaces are dulled by smoothing, which is a result of solution processes with simultaneous transportation in an aqueous environment (Widdowson 1997; Woronko and Ostrowska 2009). V-shaped percussion cracks occur on dulled surfaces, and are also particularly important in the samples taken from a distal part of the sandur and supraglacial setting. Occurrence of V-shaped cracks reveals dependence on the high-energetic fluvial environment (Bull 1986; Mahaney and Kalm 2000; Mahaney 2002; Costa *et al*. 2012; Vos *et al*. 2014), where mixing and sorting by flowing meltwater prevail (Clarhäll 2011). Apparently, percentage of grains, which display V-shaped cracks in the proximal part of the sandur is twice smaller than in the coversand located in its distal part, and is, therefore, similar with a level of such cracks in subglacial sediments in Antarctica (Mahaney *et al*. 1996) and in Norway (Hart 2006). Given that such difference is pronounced on sediments taken from

proximal and distal part of the sandur, this may be an evidence for fluvial overprint by the meltwater, which has not been recorded by expected increase of grains with shiny surface.

Aeolian signal. — Close to the ice margin strong katabatic winds combined with steep pressure gradients may develop (Brookfield 2011), thus increasing wind speed (Dijkmans and Törnqvist 1991) and enhancing aeolian activity (Müller *et al*. 2016). It is supported by results from samples taken near the ice margin. For example, among sediments representing lake shorelines and supraglacial debris, aeolian-induced grains of different rounding occur in both investigated fractions (Fig. 6E). Also landform record, seen as a presence of low-relief embryonic dunes, shapeless coversands and small-scale aeolian features (Engels and Helmens 2010), supports aeolian activity (Willemse *et al*. 2003). In this study, the embryonic dunes and coversands are particularly widespread in the distal part of the sandur plains, although aeolian cover is found in other locations as well. However, the overall grain outline in sediments of the embryonic dune does not reveal an aeolian signal in the 0.5–1.0 mm fraction, and only 4% of grains has matt surface. Subsequently, sediments taken from the rest of aeolian landforms carry more aeolian-induced grains, but only as high as 17% (in the echo dune). Such suites prove valuable for assessing as observed in many aeolian palaeoenvironments (Mycielska-Dowgiałło 1993; Narayana *et al*. 2010; Kalińska-Nartiša *et al*. 2016). In this study, sandur floodplains, ice surface and marginal moraines offer a potential source for aeolian processes. Therefore, a lack of aeolian signal in the embryonic dune can be explained by the general statement that aeolian sands derived from glacial-like source are more immature and have less rounded grains than warmer climate aeolian sands, where sand is often transported for much longer distances (Brookfield 2011). In contrast, in the Russell Glacier and proglacial area, a considerable transport distance during aerial suspension is valid for the finer sediment particles such as silt (Clarhäll 2011). Thin cover of silty aeolian deposits seems common in the Sandflughtdalen, and the high influx was periodically present in the Holocene (Willemse *et al*. 2003). Aeolian samples in this paper are much sandier with silt fraction up to 4% (unpublished data), and, therefore, aerial suspension appears not relevant.

Apparently, aeolian-induced grains significantly increase in the 1.0–2.0 mm fraction (Fig. 4). For example, rounded grains (the third and fourth classes) with matt surface have been found in the supraglacial debris and lake shoreline settings. These grains were likely rounded in aquatic environment and further their surface became matt due pushing and rolling by strong wind. Consequently, more aeolian-induced grains occur in the 1.0–2.0 mm in the sediments of the embryonic and echo dunes, which gained the strongest aeolian abrasion, possibly due to changes in transportation, as observed in some aeolian palaeoenvironments (Dzierwa and Mycielska-Dowgiałło 2003; Mycielska-Dowgiałło and Woronko

2004). It is also known that such aeolian grains are practically absent in the palaeosandur sediments (Górska-Zabielska 2015; Woronko *et al*. 2015b); however, occasionally occur in localities where longer-lasting aeolian processes under periglacial conditions took place (Kalińska-Nartiša *et al*. 2015; Woronko *et al*. 2015a). This latter is likely a case at the Russell Glacier setting.

Conclusions

Our set of quartz grain textural and microtextural properties provides signature on modern glacial environment at the Russell Glacier, South West Greenland. We debate whether the investigated quartz grains, taken from the debris sand fraction, reveal glacial characteristics and to what extend these grains carry a signal of another sedimentary settings.

What appears from the grain texture is both glacial fracturing and glacial abrasion seen as grain angularity or grain with a different level of abrasion; our two investigated sand fractions reveal such grain suite. However, the occurrence frequency of glacially induced microtextures anticorrelates with the most recognisable glacial features. Our result shows that signal coming from the fluvial environment is much stronger, than recorded by the glacial environment, potentially revealing subglacial fluvial transport. Minor fracturing and abrading point, therefore, at reduced shear stress in the marginal part of the glacier and presence of pressurized water at the ice-bed. Only abundant chemically induced microtextures served as evidence for glacial influence.

Dynamic fluvial regime produces grains with features attributable to the energetic water currents, especially in the sandur plain sediments. However, we have not detected fluvial grain transformation towards distal part of the sandur likely due to short transport distance.

A growing number of aeolian-induced grains among the samples closest to the ice margin support a theory about enhancing aeolian activity that is triggered by strong katabatic winds. In contrast, sediments of dunes and coversands aeolian grains only occur in the larger fraction that points at changes in transportation mode and a stronger aeolian abrasion.

References

AALTONEN I., DOUGLAS B., FRAPE S., HENKEMANS E., HOBBS M., KLINT K.E., LEHTINEN A., LIL-JEDAHL L.C., LINTINEN P. and RUSKEENEMI T. 2010. The Greenland Analogue Project, Sub-Project C: Field and Data Report. *Posiva Working Report* 2010-62: 135 pp.

ADAM W.G. and KNIGHT P.G. 2003. Identification of basal layer debris in ice-marginal moraines, Russell Glacier, West Greenland. *Quaternary Science Reviews* 22: 1407–1414.

BALTRUNAS V., SINKUNAS P., KARAMZA B., DUNDULIS A., CESNULEVICIUS A., KAZAKAUSKAS V., SEIRIENE V., KUKYTE D. and JANUSEVICUTE E. 2008. Till as natural isolating cover and its sedimentation in glacial environment. *In: Environmental Engineering, The 7th International Conference*. Vilnius, Lithuania: 65–70.

BROOKFIELD M.E. 2011. Aeolian processes and features in cool climates. *Geological Society, Special Publications* 354: 241–258.

BULL P.A. 1986. Procedures in environmental reconstruction by SEM analysis. *In: The Scientific Study of Flint and Chert. Fourth International Flint Symposium*. Brighton: 221–226.

CAILLEUX A. 1942. Les actiones éoliennes périglaciaires en Europe. *Mémoires de la Société Géologique de France* 41: 1–176.

CAILLEUX A. 1952. Morphoskopische Analyse der Geschiebe und Sandkörner und Ihre Bedeutung für die Paläoklimatologie. *Geologische Rundau* 40: 11–19.

CAPPELEN J., JØRGENSEN B.V., LAURSEN E.V., STANNIUS L.S. and THOMESEN R.S. 2001. *The Observed Climate of Greenland, 1958–99 with Climatological Standard Normals, 1961–90. Technical Report* 00-18: 151 pp.

CARRIVICK J.L., YDE J., RUSSELL A.J., QUINCEY D.J., INGEMAN-NIELSE T. and MALLALIEU J. 2016. Ice-margin and meltwater dynamics during the mid-Holocene in the Kangerlussuaq area of west Greenland. *Boreas* 46: 369–387.

ČESNULEVIČIUS A. and ŠEIRIENĖ V. 2009. Transformation of landforms and sediments in the periglacial setting of West Greenland. *Geologija* 51: 33–41.

ČESNULEVIČIUS A., ŠEIRIENĖ V., KAZAKAUSKAS V., BALTRŪNAS V., ŠINKŪNAS P. and KARMAZA B. 2009. Morphology and sediments of ice-dammed lake after its outburst, West Greenland. *Geologija* 51: 42–52.

CLARHÄLL A. 2011. *SKB Studies of the Periglacial Environment: Report from Field Studies in Kangerlussuaq, Greenland 2008 and 2010*. Swedish Nuclear Fuel and Waste Managment Co. P-11-05. 49 pp.

COOK S.J., GRAHAM D.J., SWIFT D.A., MIDGLEY N.G. and ADAM W.G. 2011. Sedimentary signatures of basal ice formation and their preservation in ice-marginal sediments. *Geomorphology* 125: 122–131.

COSTA P., ANDRADE C., FREITAS M., OLIVEIRA M., LOPES V., DAWSON A., MORENO J., FATELA F. and FATELA F. 2012. A tsunami record in the sedimentary archive of the central Algarve coast, Portugal: Characterizing sediment, reconstructing sources and inundation paths. *The Holocene* 22: 899–914.

DIJKMANS J.W.A. and TÄRNQVIST T.E. 1991. Modern periglacial eolian deposits and landforms in the Søndre strømfjord area, West Greenland and their palaeoenvironmental implications. *Geoscience* 25: 1–39.

DZIERWA K. and MYCIELSKA-DOWGIAŁŁO E. 2003. Reconstruction of the dynamics of aeolian processes and of their duration on the basis of selected textural features of the deposits withint the dune at Cięciwa, eastern Poland. *Przegląd Geologiczny* 51: 163–167 (in Polish).

ENGELS S. and HELMENS K. 2010. *Holocene Environmental Changes and Climate Development in Greenland*. Swedish Nuclear Fuel and Waste Managment Co. R-10-65: 40 pp.

FORMAN S.L., MARIN L., VAN DER VEEN C., TREMPER C. and CSATHO B. 2007. Little ice age and neoglacial landforms at the Inland Ice margin, Isunguata Sermia, Kangerlussuaq, west Greenland. *Boreas* 36: 341–351.

FUNDER S. and HANSEN L. 1996. The Greenland ice sheet – a model for its culmination and decay during and after the last glacial maximum. *Bulletin of the Geological Society of Denmark* 42: 137–152.

GOBALA KRISHNAN N., NAGENDRA R. and ELANGO L. 2015. Quartz surface microtextural studies of Cauvery River sediments, Tamil Nadu, India. *Arabian Journal of Geosciences* 8: 10665–10673.

GOUDIE A. and BULL P.A. 1984. Slope process change and colluvium deposition in Swaziland: An SEM analysis. *Earth Surface Processes and Landforms* 9: 289–299.

GÓRSKA-ZABIELSKA M. 2015. Roundness and matt degree of quartz grain surfaces in (fluvio-)glacial deposits of the Pomeranian Stage (Weichselian) in northeast Germany. *Geologos* 2: 117–125.

HART J.K. 2006. An investigation of subglacial processes at the microscale from Briksdalsbreen, Norway. *Sedimentology* 53: 125–146.

IMMONEN N. 2013. Surface microtextures of ice-rafted quartz grains revealing glacial ice in the Cenozoic Arctic. *Palaeogeography, Palaeoclimatology, Palaeoecology* 374: 293–302.

JØRGENESEN A.S. and ANDREASEN F. 2007. Mapping of permafrost surface using ground-penetrating radar at Kangerlussuaq Airport, western Greenland. *Cold Regions Science and Technology* 48: 64–72.

KALIŃSKA-NARTIŠA E. and NARTIŠS M. 2016. The fan-like forms in the southern margin of the Mazovian Lowland area (Central Poland): a new high-resolution textural-timing study. *International Journal of Earth Sciences* 105: 885–903.

KALIŃSKA-NARTIŠA E., THIEL C., NARTIŠS M., BUYLAERT J.P. and MURRAY A.S. 2015. Age and sedimentary record of inland aeolian sediments in Lithuania, NE European Sand Belt. *Quaternary Research* 84: 82–95.

KALIŃSKA-NARTIŠA E., THIEL C., NARTIŠS M., BUYLAERT J.P. and MURRAY A.S. 2016. The north--eastern aeolian 'European Sand Belt' as potential record of environmental changes: a case study from Eastern Latvia and Southern Estonia. *Aeolian Research* 22: 59–72.

KALIŃSKA-NARTIŠA E., WORONKO B. and NING W. 2017. Microtextural inheritance on quartz sand grains from Pleistocene periglacial environments of the Mazovian Lowland, central Poland. *Permafrost and Periglacial Processes*: 10.1002/ppp/1943.

KARLSTROM L. and YANG K. 2016. Fluvial supraglacial landscape evolution on the Greenland Ice Sheet. *Geophysical Research Letters* 43(6): 2683–2692.

KIRSHNER A.E. and ANDERSON J.B. 2011. Cenozoic Glacial History of the Northern Antarctic Peninsula: A Micromorphological Investigation of Quartz Sand Grains. *Tectonic, Climatic, and Cryospheric Evolution of the Antarctic Peninsula* 063: 153–165.

KLEESMENT A. 2009. Roundness and surface features of quartz grains in Middle Devonian deposits of the East Baltic and their palaeogeographical implications. *Estonian Journal of Earth Sciences* 58: 71–84.

KNIGHT P.G. 1997. The basal ice layer of glaciers and ice sheets. *Quaternary Science Reviews* 16: 975–993.

KONOPINSKI D.I., HUDZIAK S., MORGAN R.M., BULL P. and KENYON A. 2012. Investigation of quartz grain surface textures by atomic force microscopy for forensic analysis. *Forensic Science International* 223: 245–255.

KRINSLEY D.H. and DOORNKAMP J.C. 1973. *Atlas of Quartz Sand Surface Textures*, 1st ed., Cambridge University Press, Cambridge: 91 pp.

LILJEDAHL L.C., KONTULA A., HARPER J., NÄALUNS J.O., SELROOS J.O., PITKÄNEN P., PUIGHOME-NECH I., HOBBS M., FOLLIN S., HIRSCHORN S., JANSSON P., KENNELL J., MARCOS N., RUSKE-

ENIEMI T., TULLBORG E.L. and VIDSTRAND P. 2016. *The Greenland Analogue Project: Final Report*. Swedish Nuclear Fuel and Waste Managment Co. TR-14-13: 142 pp.

LINDBÄCK K., PETTERSSON R., DOYLE S.H., HELANOW C., JANSSON P., KRISTENSEN S.S., STENSENG L. and FORSBERG R. 2014. High-resolution ice thickness and bed topography of a land-terminating section of the Greenland Ice Sheet. *Earth System Science Data* 6: 331–338.

MADHAVARAJU J., LEE Y.I., ARMSTRON-ALTRIN J.S. and HUSSAIN S.M. 2006. Microtextures on detrital quartz grains of upper Maastrichtian-Danian rocks of the Cauvery Basin, Southeastern India: implications for provenance and depositional environments. *Geosciences Journal* 10: 23–34.

MAHANEY W.C. 1995. Pleistocene and Holocene glacier thicknesses, transport histories and dynamics inferred from SEM microtextures on quartz particles. *Boreas* 24: 293–304.

MAHANEY W.C. 1998. Scanning electron microscopy of Pleistocene sands from Yamal and Taz Peninsulas, Ob River esturay, Nortwestern Siberia. *Quaternary International* 45/46: 49–58.

MAHANEY W.C. 2002. *Atlas of Sand Grain Surface, Textures and Applications*. Oxford University Press, Oxford: 237 pp.

MAHANEY W.C. and KALM V. 1995. Scanning electron microscopy of Pleistocene tills in Estonia. *Boreas* 24: 13–19.

MAHANEY W.C. and KALM V. 2000. Comparative scanning electron microscopy study of oriented till blocks, glacial grains and Devonian sands in Estonia and Latvia. *Boreas* 29: 35–51.

MAHANEY W.C., CLARIDGE G. and CAMPBELL I. 1996. Microtextures on quartz grains in tills from Antarctica. *Palaeogeography, Palaeoclimatology, Palaeoecology* 121: 89–103.

MAHANEY W.C., DIRSZKOWSKY R.W., MILNER M.W., MENZIES J., STEWART A., KALM V. and BEZADA M. 2004. Quartz microtextures and microstructures owing to deformation of glaciolacustrine sediments in the northern Venezuelan Andes. *Journal of Quaternary Science* 19: 23–33.

MAZUMDER A., GOVIL P., KAR R., GAYATHRI N.M. and RAGHURA M. 2017. Paleoenvironments of a proglacial lake Schirmacher Oasis, East Antarctica: Insights from quartz grain microtextures. *Polish Polar Research* 38(1): 1–19.

MORAL CARDONA J.P., GUTIÉRREZ MAS J.M., SÁNCHEZ BELLÓN A., DOMÍNGUEZ-BELLA S. and MARTÍNEZ-LÓPEZ J. 2005. Surface textures of heavy-mineral grains: a new contribution to provenance studies. *Sedimentary Geology* 174: 223–235.

MÜLLER M., THIEL C. and KÜHN P. 2016. Holocene palaeosols and aeolian activities in the Umimmalissuaq valley, West Greenland. *The Holocene* 26(7): 1149–1161.

MUZIŃSKA A. 2015. Transport conditions of mountain-surging glaciers as recorded in the micromorphology of quartz grains (Medvezhiy Glacier, West Pamir). *Geologos* 21: 89–103.

MYCIELSKA-DOWGIAŁŁO E. 1993. Estimates of Late Glacial and Holocene aeolian activity in Belgium, Poland and Sweden. *Boreas* 22: 165–170.

MYCIELSKA-DOWGIAŁŁO E. and WORONKO B. 1998. Rounding and frosting analysis of quartz sand-grain surfaces and their interpretative significance. *Przegląd Geologiczny* 46: 1275–1281 (in Polish).

MYCIELSKA-DOWGIAŁŁO E. and WORONKO B. 2004. The degree of aeolization of Quaternary deposits in Poland as a tool for stratigraphic interpretation. *Sedimentary Geology* 168: 149–163.

NANSON G.C., CHEN X.Y. and PRICE D.M. 1995. Aeolian and fluvial evidence of changing climate and wind patterns during the past 100 ka in the western Simpson Desert, Australia. *Palaeogeography, Palaeoclimatology, Palaeoecology* 113: 87–102.

NARAYANA A.C., MOHAN R. and MISHRA R. 2010. Morphology and surface textures of quartz grains from freshwater lakes of McLeod Island, Larsemann Hills, East Antarctica. *Current Science* 99: 1420–1424.

NEWSOME D. and LADD P. 1999. The use of quartz grain microtextures in the study of the origin of sand terrains in Western Australia. *Catena* 35: 1–17.

NICKLING W.G. and MCKENNA NEUMAN CH. 2009. Aeolian sediment transport. *In*: A.J. Parsons and A.D. Abrahams (eds), *Geomorphology of desert environments*. *2nd Edition*. Springer, Dordrecht: 605–622.

REFAAT A.A. and HAMDAN M.A. 2015. Mineralogy and grain morphology of the aeolian dune sand of Toshka area, southeastern Western Desert, Egypt. *Aeolian Research* 17: 243–254.

ROMÁN-SIERRA J., MUÑOZ-PÉREZ J.J. and NAVARRO-PONS M. 2013. Influence of sieving time on the efficiency and accuracy of grain-size analysis of beach and dune sands. *Sedimentology* 60: 1484–1497.

RUSSELL A.J. 1989. A comparison of two recent jökulhlaups from. *Journal of Glaciology* 35: 157–162.

RUSSELL A.J. 2007. Controls on the sedimentology of an ice-contact jökulhlaup-dominated delta, Kangerlussuaq, west Greenland. *Sedimentary Geology* 193: 131–148.

RUSSELL A.J. 2009. Jökulhlaup (ice-dammed lake outburst flood) impact within a valley-confined sandur subject to backwater conditions, Kangerlussuaq, West Greenland. *Sedimentary Geology* 215: 33–49.

RUSSELL A.J., CARRIVICK J.L., INGEMAN-NIELSEN T., YDE J.C. and WILLIAMS M. 2011. A new cycle of jökulhlaups at Russell Glacier, Kangerlussuaq, West Greenland. *Journal of Glaciology* 57: 238–246.

SCHWAMBORN G., SCHIRRMEISTER L., FRÜTSCH F. and DIEKMANN B. 2012. Quartz weathering in freeze–thaw cycles: Experiment and application to the El'gygytgyn Crater Lake record for tracing Siberian permafrost history. *Geografiska Annaler: Series A, Physical Geography* 94: 481–499.

SHRIVASTAVA P.K., ASTHANA R., ROY S.K., SWAIN A.K. and DHARWADKAR A. 2012. Provenance and depositional environment of epi-shelf lake sediment from Schirmacher Oasis, East Antarctica, vis-à-vis scanning electron microscopy of quartz grain, size distribution and chemical parameters. *Polar Science* 6: 165–182.

ST. JOHN K., PASSCHIER S., TANTILLO B., DARBY D. and KEARNS L. 2015. Microfeatures of modern sea-ice-rafted sediment and implications for paleo-sea-ice reconstructions. *Annals of Glaciology* 56: 83–93.

STORMS J.E.A., WINTER I.L., DE OVEREEM I., DRIJKONINGEN G.G. and LYKKE-ANDERSEN H. 2012. The Holocene sedimentary history of the Kangerlussuaq Fjord-valley fill, West Greenland. *Quaternary Science Reviews* 35: 29–50.

STRAND K., PASSCHIER S. and NÄSI J. 2003. Implications of quartz grain microtextures for onset Eocene/Oligocene glaciation in Prydz Bay, ODP Site 1166, Antarctica. *Palaeogeography, Palaeoclimatology, Palaeoecology* 198: 101–111.

SWEET D.E. and BRANNAN D.K. 2016. Proportion of glacially to fluvially induced quartz grain microtextures along the Rhitina river, SE Alaska, USA. *Journal of Sedimentary Research* 86: 749–761.

SWEET D.E. and SOREGHAN G.S. 2010. Application of quartz sand microtextural analysis to infer cold-climate weathering for the equatorial Fountain Formation (Pennsylvanian-Permian, Colorado, U.S.A.). *Journal of Sedimentary Research* 80: 666–677.

ŠINKŪNAS P., ČESNULEVIČIUS A., KARMAZA B. and BALTRŪNAS V. 2009. Glacigenic landform features in marginal zone of Russell and Leverett glaciers, West Greenland. *Geologija* 51(1): 23–32.

TEN BRINK N.W. 1975. Holocene history of the Greenland ice sheet based on radiocarbon-dated moraines in west Greenland. *Grønlands Geologiske Under- søgelse Bulletin* 113: 1–44.

UDAYAGANESAN P., ANGUSAMY N., GUJAR A.R. and RAJAMANICKAM G.V. 2011. Surface Microtextures of Quartz Grains from the Central Coast of Tamil Nadu. *Journal Geological Society of India* 77: 26–34.

VAN AS D., HUBBARD A.L., HASHOLT B., MIKKELSEN A.B., VAN DEN BROEKE M.R. and FAUSTO R.S. 2012. Large surface meltwater discharge from the Kangerlussuaq sector of the Greenland ice sheet during the record-warm year 2010 explained by detailed energy balance observations. *Cryosphere* 6: 199–209.

VAN GOOL J.A.M., CONNELLY J.N., MARKER M. and MENGEL F.C. 2002. The Nagssugtoqidian Orogen of West Greenland: tectonic evolution and regional correlations from a West Greenland perspective. *Canadian Journal of Earth Sciences* 39: 665–686.

VELICHKO A.A. and TIMIRIEVA S.N. 1995. Morphoscopy and morphometry of quartz grains from loess and buried soil layers. *GeoJournal* 36: 143–149.

VOS K., VANDENBERGHE N. and ELSEN J. 2014. Surface textural analysis of quartz grains by scanning electron microscopy (SEM): From sample preparation to environmental interpretation. *Earth-Science Reviews* 128: 93–104.

WHALLEY W.B. and LANGWAY J. 1978. A scanning electron microscope examination of subglacial quartz grains from camp century core, Greenland – a preliminary study. *Journal of Glaciology* 25: 125–131.

WIDDOWSON M. (ed.) 1997. *Palaeosurfaces: Recognition, Reconstruction and Palaeoenvironmental Interpretation*. Geological Society of London, *Special Publications* 120: 300 pp.

WILLEMSE N.W., KOSTER E.A., HOOGAKKER B. and VAN TATENHOVE F.G. 2003. A continuous record of Holocene eolian activity in West Greenland. *Quaternary Research* 59: 322–334.

WORONKO B. 2016. Frost weathering versus glacial grinding in the micromorphology of quartz sand grains: Processes and geological implications. *Sedimentary Geology* 335: 103–119.

WORONKO B. and OSTROWSKA M. 2009. The influence of a fluvial environment on the micromorphology of quartz grain surfaces – discussion. *In*: A. Kostrzewski and R. Paluszkiewicz (eds), *Genesis, Lithology and Stratigraphy of Quaternary Deposits* 5. UAM Press, Poznań: 605–622 (in Polish).

WORONKO B., ZIELIŃSKI P. and SOKOŁOWSKI R.J. 2015a. Climate evolution during the Pleniglacial and Late Glacial as recorded in quartz grain morphoscopy of fluvial to aeolian successions of the European Sand Belt. *Geologos* 21: 89–103.

WORONKO B., PISARSKA-JAMROŻY M. and VAN LOON A.J. 2015b. Reconstruction of sediment provenance and transport processes from the surface textures of quartz grains from Late Pleistocene sandurs and an ice-marginal valley in NW Poland. *Geologos* 21: 105–115.